Accurate Target Localization for Automotive Radar

Uysal, Faruk; Aubry, Pascal J.; Yarovoy, Alexander

DOI
10.1109/RADAR.2019.8835825

Publication date
2019

Document Version
Final published version

Published in
2019 IEEE Radar Conference, RadarConf 2019

Accurate Target Localization for Automotive Radar

Faruk Uysal, Pascal J. Aubry and Alexander Yarovoy
Microwave Sensing, Systems and Signals (MS3) group at
Faculty of Electrical Engineering, Mathematics and Computer Science (EEMCS),
Delft University of Technology, Delft, The Netherlands

***Abstract*—Automotive radars suffer from low angular estimation accuracy due to the limited number of antennas and insufficient onboard processing power. This paper addresses the single target tracking problem in automotive radar by using recently proposed MIMO-monopulse approach which blends the monopulse approach with the collocated MIMO radar. We demonstrate and compare the localization performance of the MIMO-monopulse at an automotive radar on a real-world scenario. Experiments show that MIMO-monopulse results in a better angular accuracy comparing to the conventional digital beamforming even though the low-level processing power.**

I. Introduction

Millimeter wave Frequency-Modulated Continuous-Wave (FMCW) radar has been commonly used as an automotive radar to detect the range and velocity of the targets through deramp processing. With the help of the emerging multiple-input-multiple-output (MIMO) antenna technology, it is possible to utilize larger size virtual antenna array with a reduced number of physical elements to provide the special diversity needed to exploit the angular information of targets while keeping the cost and size of each radar unit low. Despite the advantages of MIMO antenna technology, modern automobile radars still suffer from low angular estimation accuracy either low processing power or the low number of physical antenna elements.

There are different approaches for the direction of arrival (DOA) estimation as monopulse techniques (comparison of the received signals in partially overlapping beams), mechanical scanning (physically rotating antenna), spatial power spectrum measurement techniques by using a phased array antenna or a mixture of these.

Mechanical scanning approach lost attention after the development of phased array antenna since the mechanical parts are not long-term resilient. At the same time, the monopulse approach which is limited by a single target, has not been considered anymore even though its superior angular sensitivity.

For a phased array antenna, the direction of arrival estimation has been studied for decades as a field of array signal processing [1], [2] which results with the development of many DoA algorithms including parametric and non-parametric methods.

Spatial power spectrum measurement techniques like Beamforming and its varieties[3] are one of the basic and well-known DoA estimation algorithms which maximizes the output signal of an array to a specific direction using a weight vector. In addition to beamforming techniques, subspace-based methods -also known as super-resolution algorithms- such as MUSIC [4] and ESPRIT [5], can improve the estimation performance of spatial power spectrum by utilizing the eigenstructure analysis. However, there are some challenges when applying high-resolution DoA estimation algorithm for an automotive FMCW radar sensor. The major challenges can be summarized as the low number of snapshots, correlation of signals, and antenna mismatches and mutual coupling [6].

Recently, Feng at.el. propose a novel direction of arrival (DoA) estimation algorithm called 'multiple-input multiple-output (MIMO)-monopulse' by combining the monopulse approach with MIMO radar [7], [8]. They manage to visualize the monopulse response similar to digital beamforming response to exploit the angular information of multiple targets. However, the advantage of MIMO-monopulse method has not been exploited for single target tracking purpose and has not been demonstrated in real automotive radar data yet. Since monopulse is fast and accurate angle estimation algorithm which has been well developed for target tracking purposes, in this paper, we proposed a processing theme to realize MIMO-monopulse approach for single target tracking which yields better angular accuracy comparing to the traditional processing.

The rest of the paper is organized as follow: Section II starts with the background of MIMO radar and monopulse. Following, the details of angle estimation using the MIMO-monopulse method and its implementation for target localization in a tracking scenario are presented. The experimental results and discussion regarding the comparison of the proposed method and the tradition processing, are presented at Section III. Finally, a conclusion is drawn in Section IV.

II. MIMO-monopulse Target Localization

A. Multiple-Input Multiple-Output (MIMO) Radar

Current FMCW automotive radars utilize a virtual array to exploit the DoA of the targets by taking the advantage of collocated transmitters and receivers. Let assume, there are M_T transmitters and M_R receivers in a MIMO antenna array. Then, a virtual array of a size of $M = M_T M_R$ can be utilized by using transmitter $\mathbf{a}_T$ and receiver $\mathbf{a}_R$ steering vectors as

$$\begin{aligned}\mathbf{a}_T(\theta) &= \begin{bmatrix}1 & e^{j2\pi\frac{d_T}{\lambda}\sin(\theta)} & \dots & e^{j2(M_T-1)\pi\frac{d_T}{\lambda}\sin(\theta)}\end{bmatrix}^T,\\ \mathbf{a}_R(\theta) &= \begin{bmatrix}1 & e^{j2\pi\frac{d_R}{\lambda}\sin(\theta)} & \dots & e^{j2(M_R-1)\pi\frac{d_R}{\lambda}\sin(\theta)}\end{bmatrix}^T,\end{aligned} \tag{1}$$

where λ is the wavelength, d_T and d_R are the inter-element spacing of the transmitters and the receivers, respectively.

978-1-7281-1679-2/19/$31.00 ©2019 IEEE

The overall steering vector of the virtual array can be written as a Kronecker product of transmitter and receiver steering vectors,

$$\mathbf{a}(\theta) = \mathbf{a}_T(\theta) \otimes \mathbf{a}_R(\theta). \tag{2}$$

The inter-element spacing for transmitters and the receivers must be designed accordingly to avoid grating lobes in the beampattern of the virtual array. One can design a MIMO array that results with a M element virtual uniform linear array (ULA) with an inter-element spacing $d = \lambda/2$ by setting the receiver inter-element spacing to half wavelengths $d_R = \lambda/2$ and transmitter spacing to $d_T = M_R d_R$.

B. Angle estimation using MIMO-monopulse

The MIMO-monopulse technique realizes the delay-and-sum beams through digital beamforming (DBF) to precisely estimate the angle of arrival of a single target at a specific direction [9], [8], [7]. The output of beamformer for a received signal $\mathbf{x}$ can be expressed as [2]

$$y = \mathbf{w}^H \mathbf{x} \tag{3}$$

where $\mathbf{w}$ is the weighting vector and $(\bullet)^H$ is the complex conjugate transpose (Hermitian transpose).

For a phase comparison monopulse (PCM), the antenna array can be divided into two equal sub-arrays to compare the phase information. For an array of M elements, the left $M/2$ elements creates the left sub-array while the rest of the elements forms the right one [10].

For an amplitude comparison monopulse (AMC), the left and right beams are generated by two beamforming vectors centered at initial direction θ_0 but separated by a squint angle shift θ_s to left and right [11]. The weights of left and right beamformers can be written respectively as

$$\begin{aligned} \mathbf{w}_l &= \mathbf{a}(\theta_0 - \theta_s/2), \\ \mathbf{w}_r &= \mathbf{a}(\theta_0 + \theta_s/2). \end{aligned} \tag{4}$$

After beamforming, using left and right weighting vectors, the beamformer output of the two beams is compared to locate the angle of the targets.

The difference between two beams will be zero when the target is at the initial look direction θ_0, whereas the sum of two beams has its maximum value. A small offset of target's angle from the initial look direction generates an error voltage which is used to estimate the target's angle. It is possible to use the imaginary part of monopulse ratio to compute the error voltage,

$$\epsilon = \Im\left\{\frac{\mathbf{w}_\Delta^H \mathbf{x}}{\mathbf{w}_\Sigma^H \mathbf{x}}\right\} \tag{5}$$

where the sum and difference weight vectors are respectively expressed as

$$\begin{aligned} \mathbf{w}_\Delta &= (\mathbf{w}_l - \mathbf{w}_r), \\ \mathbf{w}_\Sigma &= (\mathbf{w}_l + \mathbf{w}_r), \end{aligned} \tag{6}$$

and $\Im\{z\}$ shows the imaginary part of a complex number z. Once an error voltage is computed, the angle of the target is estimated through inverse mapping. The linear approximation region of the monopulse ratio is then used to estimate the target's angle as

$$\theta_T = \theta_0 - \gamma^{-1}\epsilon \tag{7}$$

where γ is the constant slope of monopulse ratio inside the approximated linear region.

C. Implementation of MIMO-monopulse for Localization

The estimation performance of the MIMO-monopulse using (7) does not depend on any grid size thus yields a better location accuracy especially for higher angular quantization (see Sections III), but requires two steering vector compared with conventional beamforming method for angle estimation. However, new steering vector is only needed when the target is out of linear region of MRC. Thus, proposed method is computationally efficient and can be realized by using minimum number of FFT bins for single target localization/tracking purposes.

In this paper, we use Chebyshev and Zolotarev weightings together with steering vector as sum $\mathbf{w}_\Sigma$ and the difference $\mathbf{w}_\Delta$ beams, respectively to achieve a larger linear region (to satisfy the assumption constant slope γ) at MRC. Readers are referred to [8], [7] for a detailed explanation of using Chebyshev and Zolotarev weightings in MIMO-monopulse configuration.

The procedure of single target tracking is illustrated in Figure 1 with the grey flow whereas traditional processing is highlighted with blue flow. The overall processing can be summarized as following steps;

1) First a tracker requests for an accurate localization for a predetermined target at range R and angle θ_i.
2) A monopulse beam is created at angle θ_i by using digital beamforming as explained in Section II-B. Initial direction is set to angle of predetermined target $\theta_0 = \theta_i$.
3) Direction of target θ_T is estimated using linear mapping (7) and set to target location $\theta_i = \theta_T$.

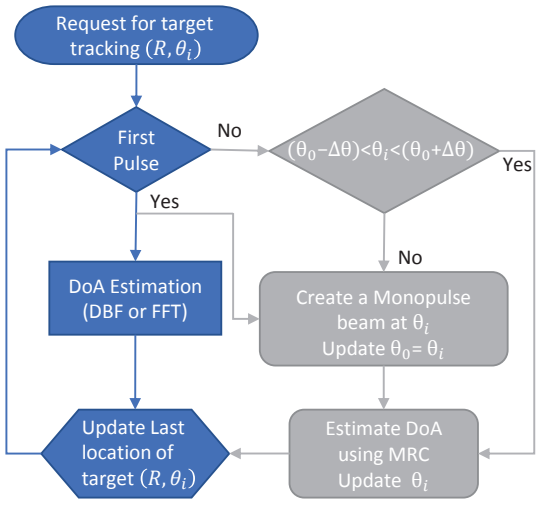

Fig. 1. Flow diagram of proposed MIMO-monopulse target tracking (grey flow) as an alternative or parallel to the tradition processing (blue flow).

978-1-7281-1679-2/19/$31.00 ©2019 IEEE

4) For the following pulses; If target is inside the linear region of MRC which is bounded by $\pm\theta_\Delta$

$$(\theta_0 - \Delta\theta < \theta_i < (\theta_0 + \Delta\theta), \tag{8}$$

estimate the direction of target using linear mapping and set the target location θ_i (Step 3). Else create a new monopulse beam (Step 2) and continue process.

III. Experiments and Discussions

For experimental verification, a new generation NXP TEF810X transceiver chip (which is designed for automotive radar applications) together with S32R274 Radar microcontroller is used to collect the real data. Transceiver chip is set to 78.8 GHz center frequency with a bandwidth of 1.0 GHz. To synthesize a 12 element virtual array, 3 transmitter and 4 receivers are used in TDMA (Time-division Multiple Access) MIMO setup. The other radar parameters (such as duration of the pulse, number of pulse, pulse-repetition time (PRT), and etc...) are set according to automotive short range radar (SRR) requirements.

Calibration of the system is not done on monopulse level. Instead, since the MIMO-monopulse realize monopulse beams through beamforming, the 12 element virtual array is calibrated accordingly by using the FMCW MIMO radar calibration and mutual coupling compensation approach at [12].

Spectral Estimation Methods vs MIMO-monopulse:

In general, spectral estimation techniques can be used to estimate the DoA from the spatial samples generated by antenna arrays. The spatial frequency resolution [13],

$$\delta\theta \approx 0.886 \frac{\lambda}{Md\cos\theta}, \tag{9}$$

is limited by the number of antennas M.

There are different spectral estimation method, such as classical Fourier Transform (FT) and Digital Beamforming (DBF), which can be used to estimate the DoA. Note that sub-spaced based methods such as MUSIC and ESPRIT are not considered in this paper and not compared with proposed method due to their high computational complexities which is not suitable for real-time automotive radar applications.

The phase difference $\Delta\phi$ in the signals received at two adjacent receivers is [14],

$$\Delta\phi = \frac{2\pi}{\lambda} d \sin\theta, \tag{10}$$

which is already taking into account by the steering array for beamforming at (1). Thus in beamforming, for a M element virtual array, each spatial frequency spectrum bin can be represented by $2\pi/M$.

For real-time processing Discrete Fourier Transform (DFT), which can be efficiently computed using Fast Fourier Transform (FFT), is used to exploit the spatial frequency spectrum as

$$X_k = \sum_{m=0}^{M-1} x_m \, e^{jk\Delta\phi} \tag{11}$$

where $k = 0, 1, ..., (M-1)$. When the length of the virtual array is a power of two, radix-2 FFT algorithms can be used to speed up processing time. If virtual array length is not a power of two, a zero padding (which simply refers to adding zeros to the end of collected signal to increase its length) is applied to increase antenna array size to the power of two. In that case, each spatial frequency spectrum bin can be represented f_s/N, where f_s is the spacial sampling frequency and N is the number of frequency bins in special frequency spectrum ($M \leq N$).

The total number of FFT bins N after zero padding affects the angle estimation accuracy. The DBF results with an equally spaced frequency grid whereas FFT processing results with an irregular grid due to

$$\theta = \arcsin\left(\frac{\lambda\Delta\phi}{2\pi d}\right). \tag{12}$$

The effect of different number of FFT bins used in DoA estimation is demonstrated in Figure 2b, 2c and 2c where the change of grid size depending to the look angle can easily be seen between figures. Observe that, the grid size is getting larger when the absolute value of look angel gets larger. This effect gets severe when N gets smaller.

The data shown in Figure 2 is collected in a real world scenario where a car is moving in a parking lot with a speed of 10 km/h. A video[1] frame is shown in Figure 2a where a bike passing across is selected as a target of interest, at 30° relative to the line-of-side of the radar. Figure 2b, 2c and 2d show the outputs of FFT processing (estimated DoA) for different range between 8m to 11m, when number of FFT bins is set to 16, 32 and 64, respectively. Green dot shows the maximum of the FFT output for the local region as the estimated direction for the target of interest and MIMO-monopulse output is shown with black dot. Note that MIMO-monopulse output is independent from the grid (grid is indicated with black lines in the image) whereas FFT output is always in the grid. Estimated target location for each case is summarized at Table I. As seen from the table, traditional FFT processing results suffer from the different grid size thus yields an inaccurate result for each case whereas MIMO-monopulse results have similar outputs. Even though, the MIMO-monopulse outputs also slightly deviate from expected target's location (because of the initial look direction θ_0 for each case is different due to the continuous tracking), the MIMO-monopulse performs better than the traditional FFT processing.

TABLE I
Estimated target location for the case shown at Figure 2

	Nfft=16	Nfft=32	Nfft=64
FFT Processing	34.85°	32.23°	28.94°
MIMO-monopulse	30.24°	30.28°	30.51°

To demonstrate the success and advantages of the proposed method in continuous localization (which provides localization

[1]Example videos for along and cross track bikes, together with processing can be seen at https://youtu.be/MVojrnpFlfQ.

978-1-7281-1679-2/19/$31.00 ©2019 IEEE

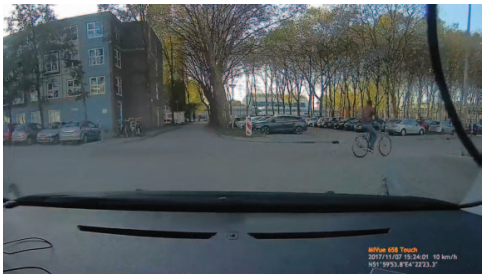

(a) Video snapshot of the data collection.

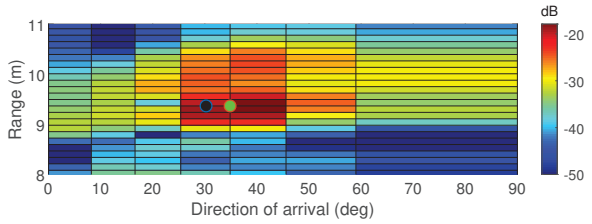

(b) Processing with $N = 16$

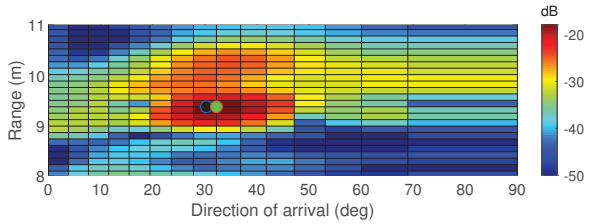

(c) Processing with $N = 32$

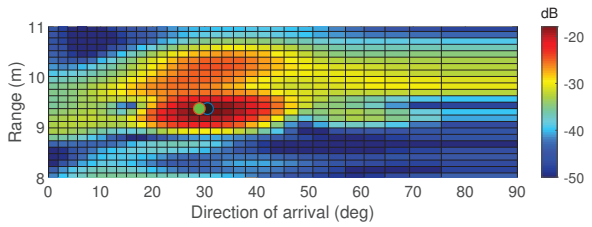

(d) Processing with $N = 64$

Fig. 2. Comparison of processing with different size FFT. Green dot shows the FFT output which is always on the grid (black lines shows the grid). Black dot shows the MIMO-monopulse output which is independent from the grid.

data to a target tracker), a controlled experiment is set up in the lab environment under the assumption of a stationary radar system. A corner (trihedral) reflector (0 dBm^2 at 77 GHz) is used as a moving target. A single target is selected for tracking and its initial range and angle (R_i, θ_i) are provided to the system. 1024 pulses (burst) is collected and processed both using FFT and the MIMO-monopulse methods simultaneously as explained in the Figure 1.

Figure 3 shows the result of both MIMO-monopulse and threditional FFT processing for different length of frequency bins N. For all sub-figures, Figure 3a, 3b and 3c, MIMO-monopulse output is illustrated by red lines and traditional FFT processing result is shown by blue lines. Black dashed lines show the scan angles of monopulse.

During the processing, for each scan angle two steering vector (size of M) together with sum and difference beam weights are used to create two monopulse beams. Between two scan angles, the target location is computed efficiently using linear mapping (7) after computing error voltage (computational complexity of MIMO-monopulse: $\mathcal{O}(M)$) for each pulse whereas a length N FFT (computational complexity: $\mathcal{O}(N \log N)$) is computed to estimate the target's angle for traditional processing. Moreover, it can easily seen from the Figure 3 that MIMO-monopulse outperforms and not affected by angular grid.

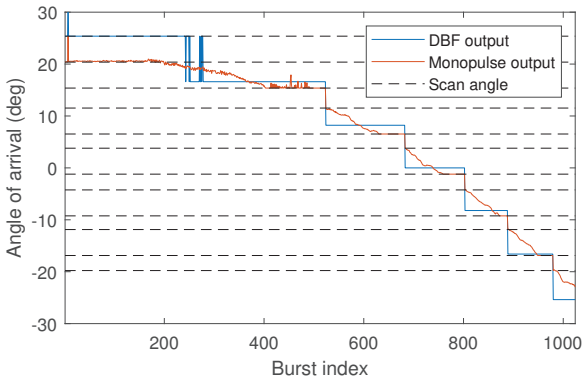

(a) Processing with an FFT length 16

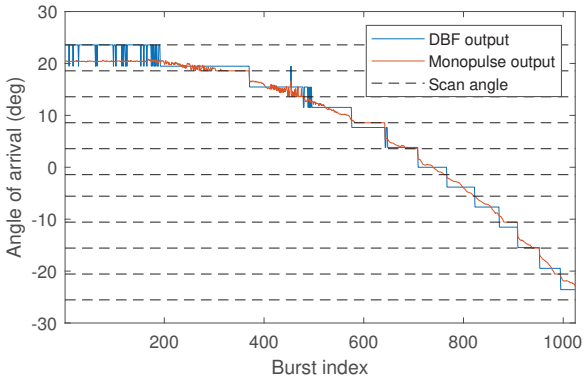

(b) Nfft = 32

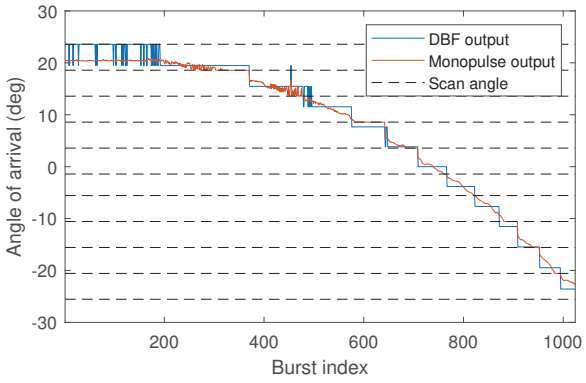

(c) Nfft = 64

Fig. 3. Result of an indoor experiment single target localization. Blue line is the traditional FFT processing. Red line is the MIMO-Monopulse poutput. Dashed black lines show the scan angles for realizing monopulse.

978-1-7281-1679-2/19/$31.00 ©2019 IEEE

IV. Conclusion

In this paper, we present an alternative method for single target localization for automobile radar tracking applications. The proposed processing theme uses the foundation of MIMO-monopulse which can be implemented parallel and synchronously to the traditional FFT processing.

We demonstrate the success of the proposed processing theme with different examples including a real-world scenario for cyclist detection and localization. Experiments show that the proposed method outperforms for a single target localization due to the independence from the frequency grid, even the number of FFT bins used for processing is limited. Thus, the proposed processing method has a definite potential to be used in real-time applications which can reduce the requirements of the microcontroller for accurate processing.

Acknowledgment

The authors would like to thank NXP Semiconductors N.V for providing the 77GHz radar transceiver with integrated radar MCUs and pointing out various technical challenges during the course of the work presented here.

References

[1] S. U. Pillai, *Array signal processing*. Springer Science & Business Media, 2012.

[2] H. L. Van Trees, *Optimum array processing: Part IV of detection, estimation, and modulation theory*. John Wiley & Sons, 2004.

[3] J. Capon, "High-resolution frequency-wavenumber spectrum analysis," *Proceedings of the IEEE*, vol. 57, no. 8, pp. 1408–1418, Aug 1969.

[4] R. O. Schmidt, "A signal subspace approach to multiple emitter location and spectral estimation," Ph.D. dissertation, Stanford University, California, 1981.

[5] R. Roy and T. Kailath, "ESPRIT-estimation of signal parameters via rotational invariance techniques," *IEEE Transactions on Acoustics, Speech, and Signal Processing*, vol. 37, no. 7, pp. 984–995, 1989.

[6] M. Schoor and B. Yang, "High-resolution angle estimation for an automotive FMCW radar sensor," in *Proc. Intern. Radar Symposium (IRS)*, 2007.

[7] R. Feng, F. Uysal, P. Aubry, and A. Yarovoy, "Mimo-monopulse target localization for automotive radar," *IET Radar, Sonar & Navigation*, August 2018.

[8] R. Feng, F. Uysal, and A. Yarovoy, "Target localization using MIMO-Monopulse: Application on 79 GHz FMCW automotive radar," in *2018 European Radar Conference (EURAD)*, Sep 2018.

[9] Q. Zhu, S. Yang, R. Yao, and Z. Nie, "Direction finding using multiple sum and difference patterns in 4d antenna arrays," *International Journal of Antennas and Propagation*, 2014.

[10] J. Zhang, H. Liu, J. Li, and C. Han, "Research on the mono-pulse phase comparison angle measurement algorithm of mimo radar," in *International Workshop on Microwave and Millimeter Wave Circuits and System Technology (MMWCST)*. IEEE, 2012, pp. 1–4.

[11] C. An, J. Yang, R. Ran, U. Y. Pak, Y.-J. Ryu, and D. K. Kim, "Enhanced monopulse MIMO radar using reliable α β filtering," in *Military Communications Conference, 2012-MILCOM*. IEEE, 2012, pp. 1–6.

[12] C. M. Schmid, C. Pfeffer, R. Feger, and A. Stelzer, "An fmcw mimo radar calibration and mutual coupling compensation approach," in *2013 European Radar Conference*, Oct 2013, pp. 13–16.

[13] M. I. Skolnik, *Introduction to radar systems, McGraw-Hili book company*. Inc, 1962.

[14] M. A. Richards, *Fundamentals of radar signal processing*. Tata McGraw-Hill Education, 2005.